



## Coulomb Stress Analysis in Nemrut Caldera (Eastern Anatolia, Türkiye)

Hamdi ALKAN<sup>1\*</sup>, Özcan BEKTAŞ<sup>2</sup>, Aydın BÜYÜKSARAÇ<sup>3</sup>

<sup>1</sup>Engineering Faculty, Department of Geophysics, Van Yüziüncü Yıl University, Van, TR

<sup>2</sup>Engineering Faculty, Department of Geophysics, Sivas Cumhuriyet University, Sivas, TR

<sup>3</sup>Çan Vocational School, Çanakkale Onsekiz Mart University, Çanakkale, TR

(ORCID: [0000-0003-3912-7503](https://orcid.org/0000-0003-3912-7503)) (ORCID: [0000-0001-5232-4654](https://orcid.org/0000-0001-5232-4654)) (ORCID: [0000-0002-4279-4158](https://orcid.org/0000-0002-4279-4158))



**Keywords:** Coulomb Stress, **Abstract**

Nemrut Caldera, Earthquake Activity, Volcano.

In volcanic areas, seismic events with low energy occur before earthquake activity or due to the movement observed in the magma. These earthquakes, which are caused by the expansion-contraction movement that has been revealed in different studies and is mostly observed in the magma chamber, can be recorded with continuous observations. On the other hand, it is not easy to distinguish between tectonic and volcanic origins of earthquakes occurring in volcanic areas. In this study, Coulomb stress analysis was carried out using earthquakes in the Nemrut Stratovolcano, which is located in eastern Anatolia and is at the westernmost end of a volcano arc. The results demonstrate a very good correlation between positive Coulomb stress changes and earthquake hypocentre depths. It was concluded that the stress is related to the Nemrut Caldera, therefore the positive stress caused by the expansion of the magma chamber of the Nemrut Volcano creates tremors.

### 1. Introduction

Eastern Anatolia region is mostly represented by volcanic rocks, mainly due to the large Quaternary volcanic centers such as Nemrut, Süphan, Tendürek, and Ağrı Mountains (Figure 1a). Nemrut Stratovolcano is one of the important volcanoes in the Eastern Anatolia located at its westernmost tip and is on the western shore of the Lake Van called the largest lake in Türkiye. Nemrut Stratovolcano started volcanic activity about 1 million years ago and was last active in 1692 [1-4]. Nemrut Stratovolcano is one of the few volcanic mountains in Türkiye that has no activity however is defined as a dormant volcano. The caldera apex of the volcano is ~2948 m in elevation, and its base is about 17 km in diameter [5]. Nemrut Caldera, the largest of which covers an area of 12.5 km<sup>2</sup> and has a freshwater lake with a depth of around 135 m and four lakes of different sizes, is the largest caldera in Türkiye [1]. The region where the Nemrut Caldera is located is also very close to the area where the Arabian Plate thrusts the Anatolian Plate, and it is a very important region in terms of tectonism. Depending on the closure of the Tethys between the

Eurasian and Arabian Plates, a thrust towards Anatolia started along the Bitlis-Zagros Suture Belt (BZSB) from the Middle Miocene, and Eastern Anatolia rose with a mean elevation of ~2 km and took the form of a plateau [5, 6]. Therefore, this system is at the source of the volcanism in Eastern Anatolia. The volcanic material started to rise along the opening cracks that started in the N-S direction and led to the development of Plio-Quaternary volcanoes [7, 8].

It was observed continuously between 2003 and 2005 with three seismometers placed around the Nemrut Caldera and the volcanic tremors recorded. These volcanic earthquakes were caused by magma activity mostly occurring at a depth of 4-5 km [1]. The depths of the crystallized and solidified deep rock masses were determined by the inversion and normalized full gradient (NFG) techniques from the air magnetic anomalies of the region where the Nemrut Caldera was located at a depth of 4-5 km. It was suggested that a magma chamber may be found at this depth [4]. The power spectrum analysis performed to estimate the deeper magnetic sources affected by hydrothermal fluids and Fe-rich rocks

\*Corresponding author: [hamdialkan@yyu.edu.tr](mailto:hamdialkan@yyu.edu.tr)

Received: 29.05.2024, Accepted: 18.07.2024

described almost the same depths. This depth range was also associated with volcanogenic earthquakes occurring at 4-5 km depth [4].

The volcanic products that form on the volcanic basement are classified into pre-caldera, syn-caldera, and post-caldera phases in the region. The basaltic trachyandesitic lava flows and peripheral silicic domes were observed in the pre-caldera activity of the Nemrut Stratovolcano. During the syn-caldera stage, explosive eruptions occurred and produced pyroclastic deposits. On the contrary, the basaltic-rhyolitic effusive activity appeared in the post-caldera activity. The post-caldera stage produced

peralkaline-type rocks, ash eruptions, and rift activities with basalt- and rhyolite-type lava flows. The last activities of Nemrut Mountain were recorded in 1441, 1597, and 1692 [5-9]. These activities refer to shallower magma chambers around a depth of 4-5 km [1, 2]. Nemrut Stratovolcano has hosted various rock groups from the Paleozoic to the present. Especially Quaternary volcanics cover a large area around the volcano. On the other hand, while Neogene units in the north and Paleogene units in the south are present, Triassic volcanics are situated to the west. On the other hand, Holocene and Quaternary faults are observed to the north and northwest of the Nemrut volcano (Figure 1b).

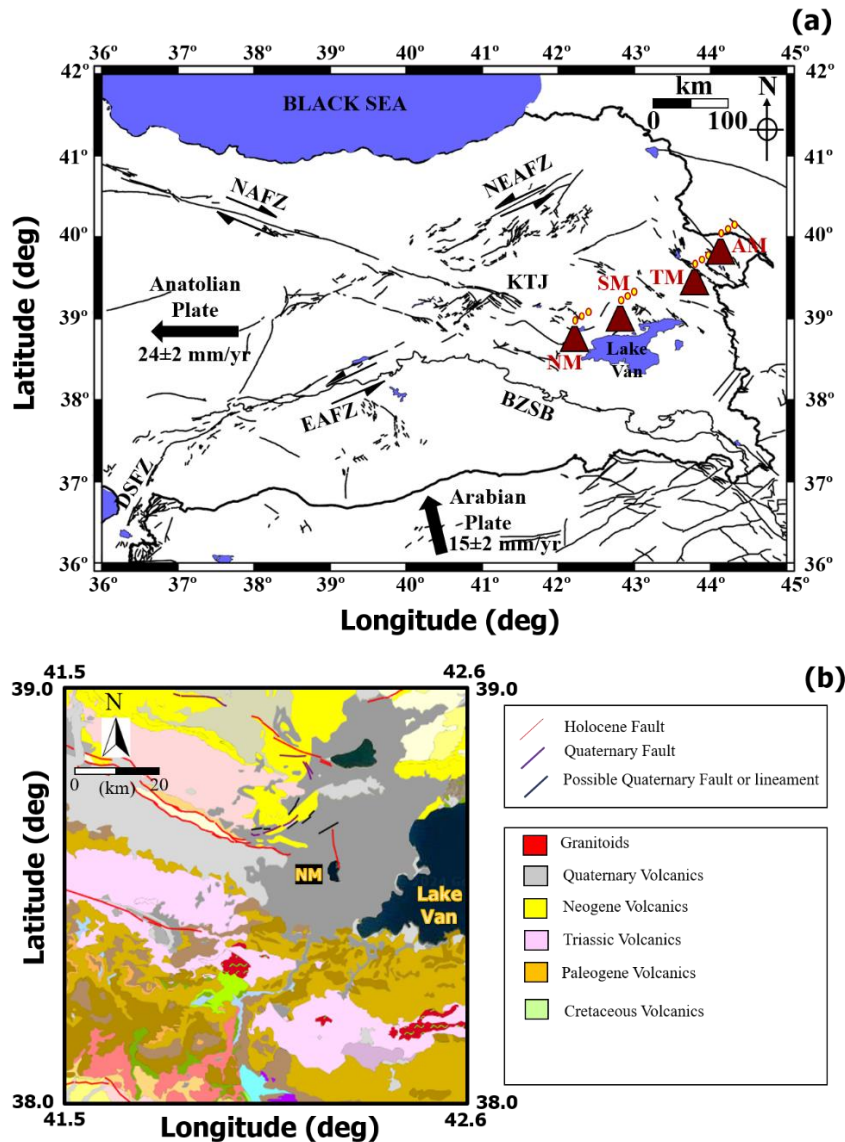


**Figure 1.** (a) Main tectonic elements of Eastern Anatolia (modified from [6, 24, 25]). Claret red triangles depict Quaternary volcanic centers. Black arrows show plate motions (taken from [26]). The solid black lines represent the active faults modified by [27, 28]. Abbreviations; AM: Ağrı Mountain, BZSB: Bitlis-Zagros Suture Belt, DSFZ: Dead Sea Fault Zone, KTJ: Karlıova Triple Junction, NAFZ: North Anatolian Fault Zone, NEAFZ: North East Anatolian Fault Zone, NM: Nemrut Mountain, SM: Süphan Mountain, TM: Tendürek Mountain. (b) The geological map of Nemrut Mountain and its surroundings [27, 29]

In literature, many studies have investigated the relationship between volcanic activity and local seismicity [10-18]. Recently, [19] used seismic data from 2003 to 2017 to describe subsurface fault structures related to volcanism and crustal tectonics in the Aleut volcanic arc near Tanaga Island. They concluded that all four volcanic centers on the island exhibited volcanic seismic activity since the observations began in 2003. Volcán de Fuego in Guatemala created a violent eruption with little warning on June 3, 2018. It created pyroclastic density currents affecting nearby settlements. This resulted in 169 deaths, 256 disappearances and approximately 13,000 people permanently displaced from their homes. It was observed with an extensive network of seismic and infrared sensors [20]. Using both seismic and infrasound data, [21] and [22] quantitatively modeled the source properties of seismo-acoustic signals associated with eruptions at Mount Cleveland in the United States and Mount Santiaguito in Guatemala, respectively.

Seismicity in volcanic regions is mainly caused by the dynamic interaction of molten rock and hydrothermal fluids with solid host rock, the fracturing and disintegration of the magma itself, and tectonic processes interacting with the volcano. [23] examined the relationships between the circulation of hydrothermal fluids, travertine precipitation, and tectonic activity. They particularly revealed the role of faults in controlling the uplift of fluids, the location of thermal sources, and the accumulation of travertine masses. Within the scope of this study, recent micro-earthquakes that occurred near the Nemrut Caldera were examined, and whether these earthquakes could be due to the pressure effects in the magma chamber or not, depending on the Coulomb stress changes.

## 2. Seismicity of Nemrut Caldera

In volcanic regions, it is necessary to discriminate between seismic activity created by tectonic processes and triggered by fluid dispersal. A full-time history analysis of the seismicity preceding and accompanying volcanic eruptions is required to understand the interaction between tectonic and magmatic processes [30]. Although the current activity of Nemrut Caldera is revealed as hot springs, fumaroles, and a small, hot lake [8], there are significant Holocene/Quaternary active fault systems around the Nemrut stratovolcano (Figure 2) [4]. In the region, the Nemrut extensional fissure is associated with the normal fault mechanism and is considered an active structural feature causing Quaternary volcanic activities in the region [28]. In addition to this, the

Nazik Gölü Fault is located in the west of the Nemrut stratovolcano and has a right-lateral strike-slip mechanism. In the west of the Nemrut Stratovolcano, the Muş Fault Zone is accompanied by a thrust-reverse character [28]. In the east of Nemrut Stratovolcano, the Southern Boundary Fault and Northern Boundary Fault are located on Lake Van.

To model the local seismicity around the Nemrut Stratovolcano, the Coulomb failure stress changes in bars should be calculated for the best-oriented focal mechanism solutions. Since the focal mechanism parameters (strike/dip/rake) of the local earthquakes around the Nemrut Caldera cannot be reached, we overcome this problem by obtaining the numerical 3-component data recorded at the Disaster and Emergency Management Authority (AFAD) broadband stations. Detailed information on permanent broadband seismic stations is shown in Table 1. Also, the locations of the broadband seismic stations employed by the AFAD are demonstrated in Figure 2. For fault plane solutions, we perform the Seisan software package [31], which is composed of different programs such as FPFIT [32] and PINV [33]. FPFIT uses first-motion polarities for selected earthquakes based on the double-couple fault-plane solution and is the weighted sum of first-motion polarity discrepancies. It automatically finds a solution in the least squares sense, which means that it is not a correct solution however it corresponds to the best solution. FPFIT estimates the uncertainty in the model parameters (strike, dip, rake). Finally, FPFIT calculates a uniformly distributed set of solutions within the range of estimated uncertainty [32]. Besides, PINV makes an inversion with the first arrivals of all P phases selected from earthquakes and gives the best focal mechanism solution depending on P-phase polarities [32-34]. Considering the general characteristics of active fault systems around Nemrut Caldera, we state that the focal mechanism solutions of 9 local earthquakes with low magnitudes ( $1.1 \leq M_L \leq 2.9$ ) are compatible with local tectonic structures. Focal mechanism solutions calculated in this study depict generally reverse/normal fault mechanisms, consistent with the Nemrut Rift Zone in the region [5, 9]. Figure 2b and Table 2 show the selected earthquakes' locations and focal mechanisms.

**Table 1.** The broadband stations of the AFAD (TU) with detailed information in the study region were used to calculate the focal mechanism solutions

| Station Code | Latitude (°) | Longitude (°) | Elevation (m) | Opening Date |
|--------------|--------------|---------------|---------------|--------------|
| MUSM         | 38.724       | 41.511        | 1357          | 2013/03/21   |
| TVAN         | 38.524       | 43.403        | 1970          | 2001/10/20   |
| BLIS         | 38.414       | 42.115        | 1608          | 2013/03/21   |
| ADCV         | 38.808       | 42.724        | 1774          | 2011/10/28   |
| GEVA         | 38.312       | 43.058        | 1672          | 2008/11/02   |
| PERV         | 37.946       | 42.541        | 1377          | 2014/11/28   |
| SRTM         | 37.991       | 41.922        | 1145          | 2011/10/29   |
| TUTA         | 39.401       | 42.813        | 2154          | 2006/09/15   |
| DORK         | 39.387       | 42.780        | 1714          | 2017/11/09   |
| TATV         | 38.580       | 42.267        | 1831          | 2006/10/21   |
| BNGL         | 38.952       | 41.149        | 1968          | 2005/07/13   |
| BTMN         | 37.891       | 41.269        | 962           | 2010/11/25   |

**Table 2.** The fault plane solutions of the selected earthquakes based on the FPFIT and PINV Methods [33] to calculate Coulomb failure stress changes in the study region

| No | Date (day/month/year)<br>(hh:mm:ss) | Latitude<br>(°) | Longitude<br>(°) | Depth<br>(km) | Local<br>Magnitude<br>(M <sub>L</sub> ) | Dip (°), Strike (°),<br>Rake (°) | Focal Mechanism<br>Type |
|----|-------------------------------------|-----------------|------------------|---------------|---|----------------------------------|-------------------------|
| 1  | 01/01/2023 12:26:57                 | 38.657          | 42.210           | 4.4           | 1.4                                     | 71,38,-121                       | Normal                  |
| 2  | 17/11/2022 06:10:57                 | 38.624          | 42.266           | 4.6           | 2.0                                     | 13,77,-161                       | Strike-slip             |
| 3  | 28-03-2021 23:02:41                 | 38.606          | 42.242           | 4.6           | 1.1                                     | 33,45,-89                        | Normal                  |
| 4  | 30/05/2020 06:32:56                 | 38.595          | 42.249           | 4.5           | 2.0                                     | 84,88,25                         | Strike-slip             |
| 5  | 21/05/2020 20:28:52                 | 38.607          | 42.271           | 5.0           | 1.9                                     | 15,90,0                          | Strike-slip             |
| 6  | 05/03/2018 18:43:44                 | 38.604          | 42.239           | 4.6           | 1.8                                     | 29,90,0                          | Strike-slip             |
| 7  | 19/01/2018 17:41:41                 | 38.775          | 42.280           | 3.9           | 2.1                                     | 38,18,38                         | Reverse                 |
| 8  | 24/04/2015 10:13:54                 | 38.598          | 42.261           | 7.5           | 2.5                                     | 234,88,-69                       | Strike-slip             |
| 9  | 03/12/2010 11:29:34                 | 38.606          | 42.281           | 4.6           | 2.9                                     | 14,28,38                         | Reverse                 |

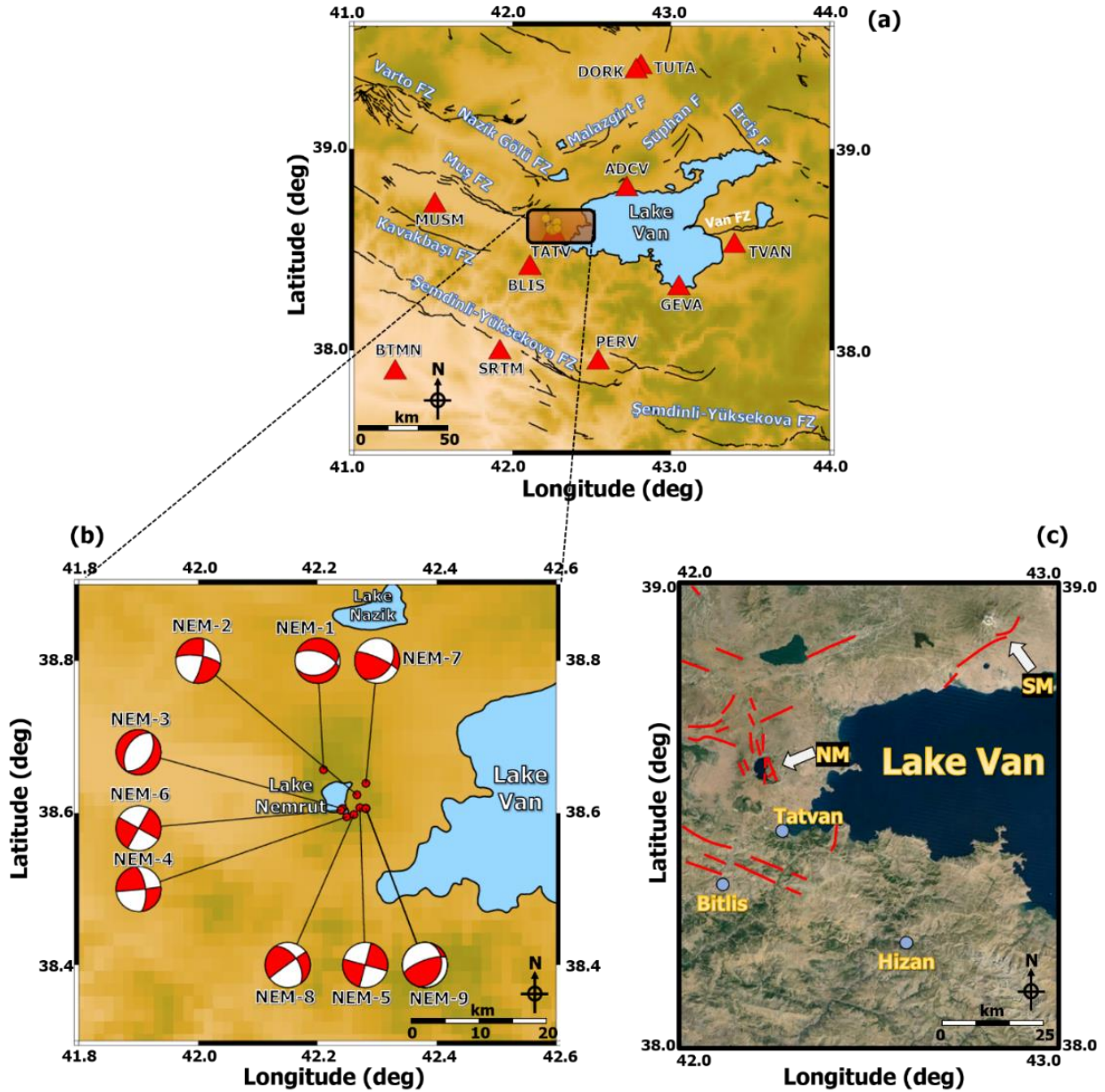


**Figure 2.** (a) Location of broadband seismic stations (red triangles). The active faults are shown with thick black lines with their names (white color) taken from [28]. The black rectangular area represents the study region. (b) The fault plane solutions and locations of the selected earthquakes (in detail please see Table 2). (c) The thick red lines depict the active faults in and around Nemrut Volcano. Blue circles represent the cities. NM: Nemrut Mountain, SM: Süphan Mountain (modified from [4])

### 3. Method of Coulomb Failure Stress Changes

Coulomb Failure stress changes ( $\Delta CFS$ ) are computed for several sources of different depths and geometry. Modeling of stress change associated with the faults slip in the tectonic regions is widely used and given information about the seismicity mechanisms [11]. In volcanic regions or non-tectonic sources such as the Nemrut Stratovolcano, it is necessary to distinguish between seismic activity generated by tectonic processes and fluid propagation.

The dip of the fault, crust rheology, the magma reservoir depth, amplitude of the pressure variation, and the nearby fault strongly influences the location of the areas of positive and negative values of Coulomb failure stress [30]. Failure occurs when the change in stress exceeds a threshold value [35, 36, 37].  $\Delta CFS$  can be defined as

$$\Delta CFS = \Delta\tau + \mu(\Delta\sigma_n + \Delta P) \quad (1)$$

where  $\Delta\tau$  and  $\Delta\sigma_n$  represent the shear stress and normal stress, respectively.  $\Delta P$  is the pore pressure

change and  $\mu$  is the frictional coefficient. According to [30], the frictional coefficient is assumed to be 0.75 associated with the viscoelastic elements of a volcano [38]. Coulomb stress changes are computed on the best-oriented fault mechanism parameters given in Table 2. Total stress change is related to the

background regional tectonic loading and the stress change resulting from the local overpressure [13]. The algorithm diagram of Seisan software and Coulomb 3.3 software is shown in Figure 3.

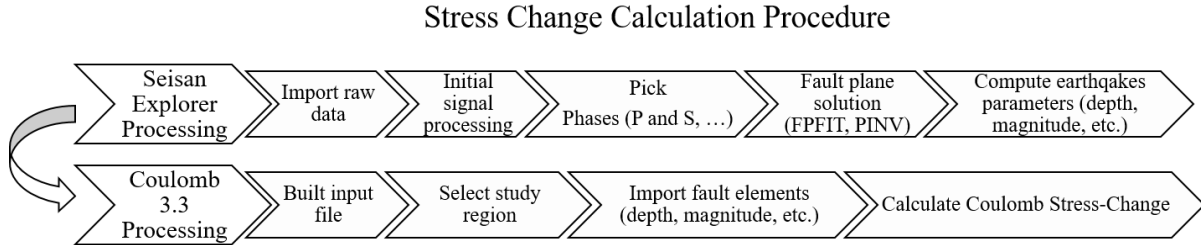


**Figure 3.** Algorithm diagram of Seisan software package [31] and Coulomb 3.3 software [37]

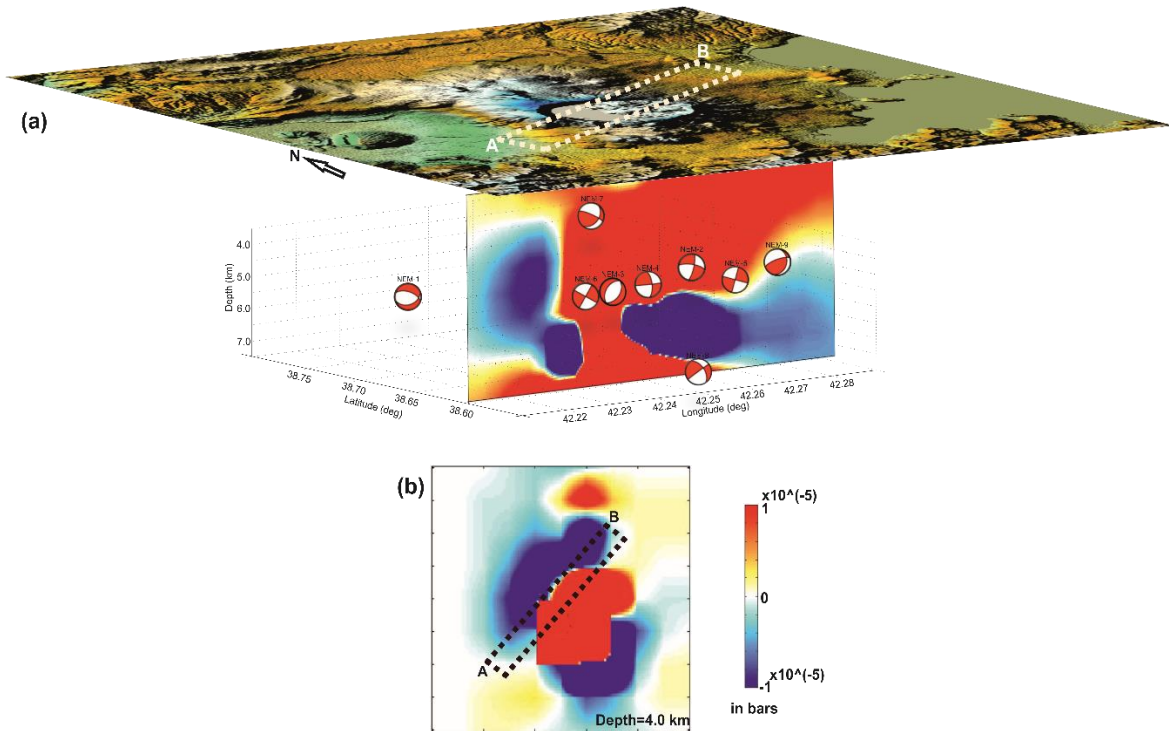


**Figure 4.** (a) 3D Topographic map around the Nemrut stratovolcano with a vertical cross-section of Coulomb failure stress ( $\Delta CFS$ ) in bars. The white dashed rectangle (line A-B) restricts the vertical cross-section with a dip angle of  $70^\circ$ . The fault friction coefficient is used as  $\mu = 0.75$ . The red beach balls belong to the focal mechanism solutions of the earthquakes given in Table 1. (b) The map of Coulomb failure stress ( $\Delta CFS$ ) at the depth of 4 km associated with all earthquakes. The black dashed rectangle depicts line A-B. The stress values are linear in the range  $-1 \times 10^{-5}$  to  $+1 \times 10^{-5}$ . Blue areas show relaxed regions, while red areas demonstrate loading regions

#### 4. Results and Discussion

This study aims to investigate the source of stress transfer and seismicity under the volcano caldera by utilizing the focal mechanism solutions of local and small earthquakes occurring around Nemrut Mountain. In Figure 4, a profile is created to cut

through the volcano caldera. According to profile A-B, both the cross-section going down to 7.5 km and the Coulomb stress change map at 4 km depth are shown. Since the deepest earthquakes with focal mechanism solutions are 7.5 km (Table 2), the cross-section is taken up to this depth. The average hypocentral depths of earthquakes are observed at a

depth of 4-5 km and these depth intervals coincide with magma chamber depth (~4 km) [4].

When we look at the cross-section, positive stress is observed in the upside and downward direction, while negative stress strikes approximately the west and east directions. At the same time, regions with positive stresses correspond to the hypocentral points of earthquakes. When the focal mechanism solutions of earthquakes are examined, it is striking that they are in the structure of strike-slip, normal faults, and oblique faults. This confirms the upward-downward stress variation. On the other hand, when the stress change at 4 km depth is examined, it can be observed that there is a similar upward positive stress. On the other hand, [39] found a Curie Point depth of approximately 17 km around the Nemrut Caldera. In the steady-state geothermal evaluation calculated using the method proposed by [40], it was predicted that a temperature of 150 °C could exist around 5 km. This corresponded to a heat flow value of approximately 90 mW/m<sup>2</sup>. However, [41] expressed the existence of an average temperature of around 1000°C. This high-temperature value was naturally associated with the pressure increase due to expansion in the caldera. Therefore, we can state that the origin of the earthquakes with irregular activity observed in the Nemrut Caldera corresponds to the expansion effects in the Caldera.

In recent years, different seismotectonic parameters such as *b*-value, *D<sub>c</sub>*-value, and Coulomb stress variation have been used by earth scientists to forecast the future seismicity for the Eastern Anatolia region. [42] investigated the seismic quiescence in the eastern part of Turkey. They identified clear quiescence anomalies at several seismogenic sources. These anomalies appeared in the Erzurum, Tunceli, Elazığ, Bingöl provinces, and Van Lake region. For these regions, they calculated the duration of quiescence before the occurrence of an earthquake as  $5.0 \pm 1.5$  years. [43] performed a statistical analysis to find out the current earthquake potential in the Eastern Anatolia region. For this purpose, he used some seismotectonic parameters called seismic *b*-value, seismic quiescence *Z*-value, cumulative moment, and annual probability and recurrence time of earthquakes. The results showed a significant decrease in *b*-value and clear quiescence anomalies in *Z*-value at the beginning of 2015 in the Central Anatolia Fault Zone, Malatya, and Ovacık faults, the southeastern part of the EAFZ, north of Lake Van, and Malazgirt Fault. These results may supply significant clues to reveal the seismic potential and trigger stress increases in the region. [44] made a similar and enhanced study for the Eastern Anatolia region based on the seismotectonic *b*-value, fractal

dimension *D<sub>c</sub>*-value, and precursory seismic quiescence *Z*-value. According to the results of [44], small *b*-values and large *D<sub>c</sub>*-values were observed in the Çaldıran Fault, around the Genç Fault, Pülümür and Karakoçan Faults, and the Sancak-Uzunpınar Fault Zone. Moderate *b*-values changing between 1.0 and 1.1 and *D<sub>c</sub>*-values changing between 2.1 and 2.2 were calculated around the Nemrut Volcano and the southern area of the BZTZ, EAFZ, and eastern area of the NAFZ. [45] made an analysis of the spatial and temporal changes of *b*-value and Coulomb stress change around the Lake Van region. For this purpose, they used a homogeneous earthquake catalog for *b*-value distribution and focal mechanism solutions of 83 local earthquakes for Coulomb stress change. They observed a decreasing trend in the *b*-values and positive Coulomb stress changes around the eastern part of Lake Van covering the Van Fault Zone, Yeniköşk Fault, Çaldıran, Başkale and Yüksekova-Şemdinli Fault Zones. On the contrary, their analysis presented the Süphan and Nemrut volcanoes did not show any significant stress change. [46] made a seismic hazard analysis of the multiple parameters in and around the Lake Van region covering the Nemrut Volcano. They used some important seismotectonic parameters such as *b*-value, *Z*-value, relative intensity (RI) and pattern informatics (PI), and Coulomb stress changes. Especially *RI-PI* algorithm in first assessed in the region. They stated that smaller *b*-values, higher *Z*-values, positive-Coulomb stress changes, and the locations of earthquake hotspots for 2022-2032 corresponded with Muradiye, Çaldıran, Özalp, Erçek, Van and Gevaş, Erciş, Malazgirt and Saray provinces. For the Nemrut Volcano and its surroundings, they calculated a higher *b*-value and positive seismic quiescence anomaly. These values generally indicated a great number of small-magnitude earthquakes. On the contrary, negative/moderate Coulomb stress values were calculated around the Nemrut Volcano. These negative Coulomb stress values and higher *b*-values indicated that tectonic earthquakes were less likely to occur in volcanic regions.

In the case of an increase in pressure of the magma reservoir or the reservoir inflation, changes in Coulomb failure stress indicate that the positive variations are most marked above and beneath the magma chamber. Therefore, seismicity and cracks may be expected to develop in this region [12]. When the pressure decreases (the reservoir deflation), the seismicity should occur laterally offset from the extent of the magma reservoir and at the same depth [30]. [13] modeled the Coulomb stress changes of Campi Flegrei Caldera due to the magma chamber overpressure and associated them with shallow

earthquake locations ( $\leq 4$  km) during magma reservoir inflation. The stress changes associated with overpressure in the shallow magma chamber were then likely to be the primary cause of local seismicity. The seismicity can be interpreted in terms of Coulomb stress changes produced by a source of overpressure, in the presence of ring faults bordering the caldera, and with a background, regional stress.

## 5. Conclusions

This study models Coulomb stress variations caused by the local seismic activity beneath the Nemrut Caldera. Coulomb stress changes have been calculated for the best-oriented focal mechanism solutions demonstrating a perfect correlation to active fault mechanisms located in the region. Results indicate that positive stress changes are oriented upward and downward striking due to the possible magma chamber and hypocenter areas. The focal mechanism depths of the earthquakes calculated in this study are compatible with the possible magma chamber depth. The magnitudes of earthquakes agree with the magnitudes of energy released during volcanic tremors. On the contrary, negative stress changes strike roughly the E-W directions. Also, the findings of this study suggest that the magma chamber beneath the Caldera plays a more relevant

role in increased stress changes. As a consequence, the activation of volcanic sources such as overpressure in the magma chambers or magma movement except tectonic seismicity may cause low-magnitude volcano-tectonic seismicity.

## Acknowledgment

The authors thank the Editor-in-Chief and the anonymous reviewers for their careful reviews and comments that improved the manuscript. We also thank the Disaster and Emergency Management Authority (<https://deprem.afad.gov.tr/>) for providing seismic. Some of the figures were created by the Generic Mapping Tools (GMT) [47]. Coulomb stress changes were calculated in Coulomb 3.3 software [37].

## Contributions of the authors

The authors' contributions to the paper are equal.

## Conflict of Interest Statement

There is no conflict of interest between the authors.

## Statement of Research and Publication Ethics

The study is complied with research and publication ethics

## References

- [1] İ. Ulusoy, *Etude volcano-structurale du volcan Nemrut (Anatolie de l'Est Turquie) et risques naturels associes*, PhD. Thesis, University of Clermont-Ferrand II, France & Hacettepe University, Turkey, 2008.
- [2] İ. Ulusoy, H. E. Çubukçu, E. Aydar, P. Labazuy, O. Ersoy, E. Şen, and A. Gourgaud, "Volcanological evolution and caldera forming eruptions of Mt. Nemrut (Eastern Turkey)", *Journal of Volcanology and Geothermal Research*, vol. 245-246, pp. 21-39, 2012.
- [3] H. E. Çubukçu, İ. Ulusoy, O. Ersoy, E. Aydar, E. Şen, A. Gourgaud, and H. Guillou, "Mt Nemrut Volcano (Eastern Turkey): Temporal petrological evolution", *Journal of Volcanology and Geothermal Research*, vol. 209-210, pp. 33-60, 2012.
- [4] Y.L. Ekinci, A. Büyüksaraç, Ö. Bektaş, and C. Ertekin, "Geophysical investigation of Mount Nemrut stratovolcano (Bitlis, Eastern Turkey) through aeromagnetic anomaly analyses", *Pure and Applied Geophysics*, vol. 177, pp. 3243-3264, 2020.
- [5] C. Ertekin, Y.L. Ekinci, A. Büyüksaraç, and R. Ekinci, "Geoheritage in a mythical and volcanic terrain: an inventory and assessment study for geopark and geotourism, Nemrut Volcano (Bitlis, Eastern Turkey)", *Geoheritage*, vol. 13, no. 3, p. 73, 2021.
- [6] F. Şaroğlu, and Y. Güner, "Doğu Anadolu'nun Jeomorfolojik Gelişimine Etki Eden Ögeler: Jeomorfoloji, Tektonik, Volkanizma İlişkileri", *Türkiye Jeoloji Kurumu Bülteni*, vol. 24, no. 2, pp. 39-50, 1981.
- [7] A. Koçyiğit, A. Yılmaz, S. Adamia, and S. Kuloshvili, "Neotectonics of East Anatolian Plateau (Turkey) and Lesser Caucasus: implication for transition from thrusting to strike-slip faulting", *Geodin Acta*, vol. 14 pp. 177-195, 2001.
- [8] İ. Ulusoy, P. Labazuy, E. Aydar, O. Ersoy, Çubukçu E., "Structure of the Nemrut caldera (Eastern Anatolia, Turkey) and associated hydrothermal fluid circulation", *J. Volcanol. Geotherm. Res.*, vol. 74 pp. 269-283, 2008.



- [9] E. Işık, M.C. Aydın, A. Bakış, and M.H. Özlük, “Bitlis ve civarındaki faylar ve bölgenin depremselliği”, *Bitlis Eren Üniversitesi Fen Bilimleri Dergisi*, vol. 1, no. 2, pp.153-169, 2012.
- [10] R. I. Tilling, and J. J., Dvorak, “Anatomy of a basaltic volcano”, *Nature*, vol. 363, pp. 125-132, 1993.
- [11] C. Troise, “Stress changes associated with volcanic sources: constraints on Kilauea rift dynamics”, *J. Volcanol. Geoth. Res.*, vol. 109, pp.191-203, 2001.
- [12] S. Toda, R. Stein, and T. Sagiya, “Evidence from the AD 2000 Izu islands earthquake swarm that stressing rate governs seismicity”, *Nature*, vol. 419, pp. 58-61, 2002.
- [13] C. Troise, F. Pingue, and G. De Natale, “Coulomb stress changes at calderas: Modeling the seismicity of Campi Flegrei (southern Italy)”, *Journal of Geophysical Research: Solid Earth*, vol. 108, no. B6, 2003.
- [14] T. R. Walter, and F. Amelung, “Influence of volcanic activity at Mauna Loa, Hawaii, on earthquake occurrence in the Kaoiki seismic zone”, *Geophys. Res. Lett.*, vol. 31, no. 7, 2004.
- [15] C. Doubre, *Structure et mecanique des segments de rift volcano-tectoniques: application aux rift anciens (Ecosse, Islande) et actifs (Asal-Ghoubbet)*, Doctoral dissertation, Université du Maine, Le Mans, France, 2004.
- [16] G. R. Foulger, B. R. Julian, D. P. Hill, A. M. Pitt, P. E. Marlin, and E. Shalev, “Non-double-couple microearthquakes at Long Valley caldera, California, provide evidence for hydraulic fracturing”, *J. Volcanol. Geoth. Res.*, vol. 132, pp. 45-71, 2004.
- [17] G. R. Foulger, J. H. Natland, and D. L. Anderson, “Genesis of the Iceland melt anomaly by plate tectonic processes. In: Plates, Plumes and Paradigms (G.R. Foulger, J.H. Natland, D.C. Presnall and D.L. Anderson, eds)”, *Geological Society of America*, Boulder, vol. 388, pp.595-626, 2005.
- [18] J. Gargani, L. Geoffroy, S. Gac, and S. Cravoisier, “Fault slip and Coulomb stress variations around a pressured magma reservoir: consequences on seismicity and magma intrusion”, *Terra Nova*, vol. 18, no.6, pp. 403-411, 2006.
- [19] K. F. Lally, J. Caplan-Auerbach, and J. A. Power, “Volcanic and tectonic sources of seismicity near the Tanaga volcanic cluster, Alaska”, *Geochemistry, Geophysics, Geosystems*, vol. 24, no. 6, 2023.
- [20] A. Diaz-Moreno, A. Roca, A. Lamur, B. H. Munkli, T. Ilanko, T. D. Pering, A. Pineda, and S. De Angelis, “Characterization of Acoustic Infrasound Signals at Volcán de Fuego, Guatemala: A Baseline for Volcano Monitoring”, *Front. Earth Sci.*, vol. 8, 2020.
- [21] A. M. Iezzi, D. Fee, M. M. Haney, and J. J. Lyons, “Seismo-Acoustic Characterization of Mount Cleveland Volcano Explosions”, *Front. Earth Sci.*, vol. 8, 2020.
- [22] A. Rohnacher, A. Rietbrock, E. Gottschämmer, W. Carter, Y. Lavallée, S. De Angelis, J. E. Kendrick, and G. Chigna, “Source Mechanism of Seismic Explosion Signals at Santiaguito Volcano, Guatemala: New Insights From Seismic Analysis and Numerical Modeling”, *Frontiers in Earth Science*, vol. 8, 2021.
- [23] A. Brogi, C. Alçiçek, C. Ç. Yalciner, E. Capezzuoli, D. Liotta, M. Meccheri, V. Rimondi, G. Ruggieri, A. Gandin, A. Büyüksaraç, H. Alçiçek, A. Bülbül, C. C. Shen, M. O. Baykara, and C. Boschi, “Hydrothermal fluids circulation and travertine deposition in an active tectonic setting: insights from the Kamara geothermal area (western Anatolia, Turkey)”, *Tectonophysics*, vol. 680, pp. 211-232, 2016.
- [24] F. Şaroğlu, O. Emre, and O. Kuşçu, “Active fault map of Turkey”, *General Directorate of Mineral Research and Exploration, Ankara, Turkey*, 1992.
- [25] E. Bozkurt, E. “Neotectonics of Turkey-a synthesis”, *Geodinamica Acta*, vol. 14, no. 1-3, pp. 3-30, 2001.
- [26] R. Reilinger, S. McClusky, P. Vernant, S. Lawrence, S. Ergintav, and R. Cakmak, “GPS constraints on continental deformation in the Africa-Arabia-Eurasia continental collision zone and implications for the dynamics of plate interactions”, *Journal of Geophysical Research*, vol. 111, no. B05411 pp. 1-26, 2006.
- [27] O. Emre, T. Y. Duman, S. Ozalp, H. Elmaci, S. Olgun, and F. Saroglu, “1/1.125.000 scale Active Fault Map of Turkey, General Directorate of Mineral Research and Explorations Special Publications Series”, Ankara-Turkey, 2013.
- [28] Ö. Emre, T. Y. Duman, S. Özalp, F. Şaroğlu, Ş. Olgun, H. Elmacı, and T. Çan, “Active fault database of Turkey”, *Bulletin of Earthquake Engineering*, vol. 16, no. 8, pp.3229-3275, 2018.

- [29] B. Akbaş, N. Akdeniz, A. Aksay, İ. E. Altun, V. Balcı, E. Bilginer, T. Bilgiç, M. Duru, T. Ercan, İ. Gedik, Y. Günay, İ. H. Güven, H. Y. Hakyemez, N. Konak, İ. Papak, Ş. Pehlivan, M. Sevin, M. Şenel, N. Tarhan, N. Turhan, A. Türkecan, Ü. Ulu, M. F. Uğuz, A. Yurtsever, and et al., “1:1.250.000 ölçekli Türkiye Jeoloji Haritası”, *Maden Tetkik ve Arama Genel Müdürlüğü Yayını*, Ankara-Türkiye, 2011.
- [30] J. Gargani, L. Geoffroy, S. Gac, and S. Cravoisier, “Fault slip and Coulomb stress variations around a pressured magma reservoir: consequences on seismicity and magma intrusion”, *Terra Nova*, vol. 18, no. 6 pp. 403-411, 2006.
- [31] L. Ottemöller, P. H. Voss, and J. Havskov, *SEISAN Earthquake Analysis Software for Windows, Solaris, Linux and Macosx*, University of Bergen, Version 12.0., 607, 2021.
- [32] P. Reasenber, and D. Oppenheimer, “Fpt, fplot, and fpage: Fortran computer programs for calculating and displaying earthquake fault plane solutions”, *Technical report*, U.S. Geol. Survey, 1985.
- [33] D. Suetsugu, “Practice on source mechanism”, iisee lecture note, *Technical report*, Tsukuba, Japan, 1998.
- [34] H. Alkan, S. Öztürk, and İ. Akkaya, “ Analysis of Coulomb stress transfer and earthquake hazard in the Çaldıran Fault Zone and its adjacent region”, *Mühendislik Bilimleri ve Tasarım Dergisi*, vol. 11, no. 2, pp. 519-534, 2023.
- [35] G. C. King, R. S. Stein, and J. Lin, “Static stress changes and the triggering of earthquakes”, *Bulletin of the Seismological Society of America*, vol. 84, no. 3, pp. 935-953, 1994.
- [36] R. Stein, “The role of stress transfer in earthquake occurrence”, *Nature*, vol. 402, pp. 605-609, 1999.
- [37] S. Toda, R. S. Stein, and J. Lin, “Widespread seismicity excitation throughout central Japan following the 2011 M=9.0 Tohoku earthquake and its interpretation by Coulomb stress transfer”, *Geophysical Research Letters*, vol. 38, no. 7, 2011.
- [38] T. Parsons, “Post-1906 stress recovery of the San Andreas fault system calculated from three-dimensional finite element analysis”, *J. Geophys. Res.*, vol. 107, 2002.
- [39] Ö. Bektaş, D. Ravat, A. Büyüksaraç, F. Bilim, and A. Ateş, “Regional Geothermal Characterisation of East Anatolia from Aeromagnetic, Heat Flow and Gravity Data”, *Pure appl. geophys.*, vol. 164, pp. 975-998, 2007.
- [40] J. H. Sass, and A. H. Lachenbruch, “Heat flow and conduction-dominated thermal regimes, Assessment of Geothermal Resources of the United States”, *United States Geological Survey Circular*, vol. 790, pp. 8-11, 1978.
- [41] I. S. Peretyazhko, E. A. Savina, and N. S. Karmanov, “Comendites and pantellerites of Nemrut volcano, eastern Turkey: Genesis and relations between the trachyte-comenditic, comenditic, and pantelleritic melts”, *Petrology*, vol. 23, pp. 576-622, 2015.
- [42] S. Öztürk, and Y. Bayrak, “ Spatial variations of precursory seismic quiescence observed in recent years in the eastern part of Turkey”, *Acta Geophys.*, vol. 60, pp. 92-118, 2012.
- [43] S. Öztürk, “Space-time assessing of the earthquake potential in recent years in the eastern Anatolia region of Turkey”, *Earth Sciences Research Journal*, vol. 21, no. 2, pp. 67-75, 2017.
- [44] S. Öztürk, “Earthquake hazard potential in the Eastern Anatolian Region of Turkey: seismotectonic b and Dc-values and precursory quiescence Z-value”, *Front. Earth Sci.*, vol. 12, pp. 215-236, 2018.
- [45] H. Alkan, and E. Bayrak, “Coulomb stress changes and magnitude-frequency distribution for Lake Van region”, *Bulletin of the Mineral Research and Exploration*, vol. 168, no.168, pp. 141-156, 2022.
- [46] S. Öztürk, and H. Alkan, “ Multiple parameter analysis for assessing and forecasting earthquake hazards in the Lake Van region, Turkey”, *Baltica*, vol. 36, no.2, pp. 133-154, 2023.
- [47] P. Wessel, J. F. Luis, L. Uieda, R. Scharroo, F. Wobbe, W. H. F. Smith, and D. Tian, “The Generic Mapping Tools version 6”, *Geochemistry Geophysics Geosystems*, vol. 20, pp. 5556-5564, 2019.